Naval Research Laboratory
Washington, DC 20375-5000

NRL Memorandum Report 6419

Megavolt, Multi-Kiloamp K_a-Band Gyrotron Oscillator Experiment

W. M. BLACK,* S. H. GOLD, A. W. FLIFLET, D. A. KIRKPATRICK,**
W. M. MANHEIMER, R. C. LEE,† V. L. GRANATSTEIN,††
D. L. HARDESTY, A. K. KINKEAD AND M. SUCY†

High Power Electromagnetic Radiation Branch
Plasma Physics Division

**Electrical and Computer Engineering Department*
George Mason University, VA 22021

***Science Applications International Corporation*
McLean, VA 22102

†*JAYCOR, Inc.*
Vienna, VA 22180

††*Electrical Engineering Department*
University of Maryland
College Park, MD 20742

March 15, 1989

SECURITY CLASSIFICATION OF THIS PAGE

ADA206271

REPORT DOCUMENTATION PAGE

Form Approved
OMB No 0704 0188

1a REPORT SECURITY CLASSIFICATION UNCLASSIFIED	1b RESTRICTIVE MARKINGS
2a SECURITY CLASSIFICATION AUTHORITY	3 DISTRIBUTION/AVAILABILITY OF REPORT Approved for public release; distribution unlimited.
2b DECLASSIFICATION/DOWNGRADING SCHEDULE	
4 PERFORMING ORGANIZATION REPORT NUMBER(S) NRL Memorandum Report 6419	5 MONITORING ORGANIZATION REPORT NUMBER(S)
6a NAME OF PERFORMING ORGANIZATION Naval Research Laboratory 6b OFFICE SYMBOL (If applicable) Code 4740	7a NAME OF MONITORING ORGANIZATION
6c ADDRESS (City, State, and ZIP Code) Washington, DC 20375-5000	7b ADDRESS (City, State, and ZIP Code)
8a NAME OF FUNDING/SPONSORING ORGANIZATION ONR & SDIO/IST 8b OFFICE SYMBOL (If applicable)	9 PROCUREMENT INSTRUMENT IDENTIFICATION NUMBER
8c ADDRESS (City, State, and ZIP Code) Washington, DC	10 SOURCE OF FUNDING NUMBERS PROGRAM ELEMENT NO / PROJECT NO / TASK NO / WORK UNIT ACCESSION NO DN153-057 DN156-218

11 TITLE (Include Security Classification)
Megavolt, Multi-Kiloamp K_a-Band Gyrotron Oscillator Experiment

12 PERSONAL AUTHOR(S)
(See page ii)

13a TYPE OF REPORT	13b TIME COVERED	14 DATE OF REPORT (Year, Month, Day)	15 PAGE COUNT
	FROM 10/87 TO 10/88	1989 March 15	32

16 SUPPLEMENTARY NOTATION

17 COSATI CODES			18 SUBJECT TERMS (Continue on reverse if necessary and identify by block number)
FIELD	GROUP	SUB-GROUP	Gyrotron, Gyroklystron, Phase-locking

19 ABSTRACT (Continue on reverse if necessary and identify by block number)

A high peak power K_a-band gyrotron oscillator experiment is reported. This experiment operated at 35 GHz in a TE_{62} mode, using a 1-1.35 MeV, multi-kiloamp beam from the VEBA pulseline accelerator. The use of an apertured anode configuration provided improved beam quality compared to earlier experiments that were carried out in a foilless diode geometry. As a result, the peak power has increased to approximately 275 MW with peak efficiencies exceeding 10%. The experimental results are in reasonable agreement with the predictions of theory.

20 DISTRIBUTION/AVAILABILITY OF ABSTRACT	21 ABSTRACT SECURITY CLASSIFICATION
☒ UNCLASSIFIED/UNLIMITED ☐ SAME AS RPT ☐ DTIC USERS	UNCLASSIFIED
22a NAME OF RESPONSIBLE INDIVIDUAL Steven H. Gold	22b TELEPHONE (Include Area Code) (202) 767-4004 22c OFFICE SYMBOL Code 4741

DD Form 1473, JUN 86 Previous editions are obsolete SECURITY CLASSIFICATION OF THIS PAGE

S/N 0102-LF-014-6603

CONTENTS

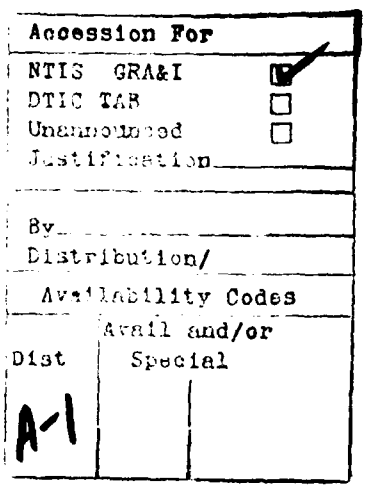

MEGAVOLT, MULTI-KILOAMP
K_a-BAND GYROTRON OSCILLATOR EXPERIMENT

I. Introduction

Gyrotron oscillators have proved to be efficient sources of very high-power radiation in the microwave and millimeter wave regimes. Conventional gyrotrons use thermionic cathodes, with typical operating currents of $\lesssim$50 A at voltages of $\lesssim$100 keV, and have demonstrated hundreds of kW of average power at efficiencies approaching 50%. However, some future applications of millimeter-wave radiation, such as radars and high energy linear electron (and positron) accelerators, may require substantially higher peak power levels than have been produced using conventional thermionic microwave tube technologies. The pursuit of higher microwave powers inevitably requires the application of higher beam powers, implying operation at higher currents and/or voltages. Gyrotron scaling to high current, high voltage operation is relatively favorable,[1] and a number of high voltage (>250 kV) gyrotron experiments have been reported in recent years that take advantage of the substantially higher currents and voltages available for short pulses (typically, $\lesssim$100 nsec) from high voltage pulseline accelerators driving plasma-induced field emission cathodes. Among these are a set of experiments from the P.N. Lebedev Physics Institute of the Soviet Union that demonstrated 23 MW at 40 GHz in a linearly-polarized (i.e., non-rotating) TE_{13} mode with 5% efficiency, using a 350 keV electron beam.[2] Studies of gyrotrons driven by pulseline accelerators or Marx generators have also been carried out at the University of Michigan[3] and at the University of Strathclyde in the United Kingdom.[4]

Manuscript approved January 24, 1989.

In 1984, a program was initiated at the Naval Research Laboratory to investigate very high power gyrotron oscillators driven by intense relativistic electron beams. These experiments were designed to operate in K_a-band, with the principal interest at 35 GHz. The early experiments were carried out on a compact Febetron pulser capable of producing a 600 kV, 6 kA, 55 nsec pulse into a 100 Ω matched load.

A key requirement for intense beam gyrotrons, unlike most other high power microwave devices driven by intense relativistic electron beams, is to produce an electron beam with a large amount of momentum transverse to the applied axial magnetic field prior to injection into the interaction region. The first series of experiments attempted to produce the required beam α, where α is the ratio of transverse to parallel momentum, by emitting electrons across magnetic field lines at the cathode to produce some initial nonzero value of α, and then adiabatically compressing the beam into the gyrotron cavity to increase α while positioning the beam to couple strongly to the desired waveguide mode. These experiments operated at approximately 350 kV and 800 A, and produced approximately 20 MW of output power at 35 GHz with 8% efficiency in a "whispering-gallery" TE_{62} mode.[5]

When this approach was found to lack flexibility, a new approach was implemented, in which the diode was designed to emit primarily along the direction of the axial magnetic field, i.e. to produce a very low initial beam α, and the α was then sharply increased by transit through a localized nonadiabatic dip in the axial field, produced by a "pump" magnet, before being adiabatically compressed into the gyrotron cavity. This allowed the use of a very simple diode geometry, and provided a separate experimental control for beam α that greatly increased the experimental flexibility.

For this second series of experiments, the Febetron pulser was operated at its full rated charge voltage and mismatched upward at the diode to produce voltages higher than 600 kV (up to 900 kV) at lower currents. Due to the high impedance of the pulser, it was impossible to employ relatively low impedance diodes, such as diodes with beam-scraper anodes, without substantially reducing the operating voltages. The experiments were therefore carried out in a foilless geometry employing a magnetic-field-immersed, cylindrical graphite cathode with a sharpened edge, in which the cylindrical vacuum vessel served as the anode. In this geometry, the diode produces a beam current determined by the space-charge limited flow of the annular beam within the cylindrical vacuum enclosure in the vicinity of the cathode. In general, this was more current than could be effectively employed in the experiment, and the use of a "pump" magnet to increase the average beam α to a level sufficient to drive the gyrotron interaction invariably resulted in the loss of a sizable fraction of the beam current. Current loss occurred due to electron mirroring during the adiabatic compression stage, due in part to the effects of beam space charge on the electron beam kinetic energy, and in part to the effects of pitch-angle spread in the beam. It was not clear exactly where the reflexing electrons were collected, or whether they caused a space-charge build-up that effected the performance of the diode.

Based on single particle simulations of the effects of the pump magnet on electrons entering with a small initial value of α and random gyrophase, it is apparent that the pump magnet has the effect of greatly magnifying any initial spread in pitch angle. Fortunately, gyrotron oscillators are not very sensitive to such pitch angle spreads. However, one result of a large electron beam pitch angle spread is to limit the average beam α achievable by this

technique, since as the strength of the pump magnet is increased, the highest α portion of the particle distribution function will be reflected during the subsequent adiabatic compression phase. Optimum high power operation generally occurred with pump strengths resulting in the loss of half or more of the total beam current between the diode and the gyrotron cavity. In addition, the diode voltage waveform was highly transient, with no true steady-state conditions of current and voltage obtainable anywhere within the pulse.

The second series of experiments was carried out in both whispering-gallery TE_{m2} modes and linearly-polarized TE_{1n} modes.[6,7] Results included a peak power of 100 MW at 35 GHz at 8% efficiency in a rotating TE_{62} mode, a peak power of 35 MW at 35 GHz in a linearly-polarized TE_{13} mode through use of a slotted gyrotron cavity. The gyrotron signal frequency could be step-tuned over the range 28 to 49 GHz in a sequence of TE_{m2} modes by variation of the axial magnetic field. Results were in general agreement with the predictions of steady-state gyrotron theory, with theoretical values of power and efficiency typically being larger than experimental values by about a factor of two. However, due to the nonideal voltage waveform provided by the Febetron pulser, the typical microwave pulse length was only 15 nsec.

In order to extend these experiments to higher microwave powers and longer pulses, as well as to gain some flexibility in the diode design in order to permit the production of a better quality electron beam, these experiments were moved to the VEBA pulseline accelerator, which can operate at voltages exceeding 1.5 MV and has a 20 Ω output impedance and a 55 nsec FWHM pulse, of which approximately 40 nsec is relatively flat ($\pm$3-5%). These new experiments initially employed a very similar experimental setup to that

utilized previously in the Febetron experiments, except that the Q=250, TE_{62} cavity of the 100 MW experiments was replaced by a slightly shorter cavity with a cold-cavity Q of 180. However, the best results have been achieved by replacing the foilless diode geometry with a beam scraper diode. By varying the cathode-anode gap, the new diode geometry has permitted control of the total current injected into the drift tube, and in addition, the more planar cathode-anode geometry is believed to produce a lower spread in the initial beam pitch angle, with the potential to produce a higher average value of α in the gyrotron cavity. Furthermore, in the new geometry, any reflexing electrons are likely to be collected on the downstream side of the beam scraper anode, thus eliminating a possible space-charge build-up problem present in the foilless experiment.

As a result of the higher beam power and improved beam quality, the output power has been increased to approximately 250 MW at 35 GHz in a TE_{62} mode with an efficiency of approximately 10%.

II. Experimental Setup

The 1.5 MeV VEBA pulseline accelerator with 20 Ω output impedance and 55 nsec voltage pulse was used to generate a multi-kiloamp annular electron beam by explosive plasma formation from a graphite cathode. Two diode geometries were employed. In the first, the electron beam was produced by emission from the sharpened edge of a cylindrical graphite anode in a simple foilless diode geometry. In the second, a more conventional planar anode-cathode gap was used, in which emission takes place from the rounded edge of a hollow cathode, and a small fraction of the total current is extracted from the diode through an

annular slot in the graphite anode. In either case, the beam is created in a uniform axial field provided by the main solenoidal magnet.

Figure 1 illustrates the overall experimental setup employing the second of these diode geometries. The initial transverse momentum is low, because the emission is predominantly along the direction of the applied magnetic field. Downstream, the transverse momentum is induced by transit through a localized depression in the axial field, which is produced by the "pump" magnet. Finally, the beam is adiabatically compressed to its final radius by the cavity solenoid. A Rogowski coil positioned between the pump magnet and the gyrotron cavity measures the net current into the gyrotron. In order to achieve separate adjustment of the electron transverse momentum, the magnetic compression ratio, and the final magnetic field in the gyrotron cavity, each of the three magnets (i.e., the pump magnet, the cavity solenoid, and the main magnet) is powered by a separate capacitor bank discharge.[6] By a proper selection of pump magnet strength and compression ratio, the beam diameter can be adjusted to couple to the desired TE_{62} mode in the cavity while the electron velocity pitch ratio α is increased to a value near unity. The cavity itself is cylindrically symmetric with a diameter of 3.2 cm and has a calculated cold-cavity Q of 180 for the TE_{62} mode. Beyond the cavity there is a 5° output taper transition to a 120 cm long drift tube with diameter of 14 cm. Finally, a one-meter-long output horn is terminated with a 32-cm-diam. output window.

In the foilless diode configuration, used in the earlier experiments, the beam current is space-charge limited with a typical value of 10 kA; however, under the usual operating conditions that maximize gyrotron microwave emission as a function of the strength of the pump magnet, only one-third of this current actually reaches the gyrotron cavity. Due to

emission from the edge of the cathode, the beam from this foilless diode possesses a relatively large spread in pitch angle, which is greatly magnified by the pump magnet. This results in a large uncontrolled loss of half or more of the beam current during the adiabatic compression, as measured by the Rogowski coil, thereby limiting the achievable pitch ratio and potentially causing space charge problems due to the reflexing electrons.

To improve the beam quality, the foilless diode was replaced by an apertured diode configuration, in which a hollow ring-like cathode is placed from 1 to 2.2 cm from an anode plate with an annulus cut in it to match the cathode ring. The mean diameter of the annulus was 3.34 cm, and its radial extent was 1.5 mm. The anode functions in part as an emittance filter, since it scrapes off the inner and outer edges of the annular electron beam produced by the cathode, and in part as a control grid, since changes in the cathode-anode gap are a reliable means to control the beam current, which is space-charge limited. A consequence of the use of an apertured anode, rather than a foilless geometry, is the emission of a large amount of cathode current (25-35 kA), with roughly 90% being scraped off before leaving the diode. However, the more planar emission geometry and the controlled beam scraping provides the beam with a lower initial α and a smaller velocity spread before it enters the pump magnet and beam compression regions. As a result, the beam quality is improved and the current loss from the diode to the cavity can be reduced to approximately 10 to 15% under typical conditions of gyrotron operation. This small fraction of reflected electrons is most likely to be collected on the downstream side of the anode scraper plate, thereby preventing a build-up of space charge anywhere in the system.

The microwave measurement system consists of two separate detection channels, each composed of calibrated "in-band" WR-28 components, including filters, attenuators and directional couplers, and beginning with a small microwave aperture antenna positioned within 1 cm of the output window. One aperture is maintained at a fixed position on the output window, while the second is scanned. A band-pass filter limits the detected signal to a narrow frequency band (1.6 GHz FWHM) centered at 35 GHz. These diagnostics as well as the overall experimental setup are described in greater detail in Ref. 6. The changes affecting the present work are in the diode region, the cavity Q, and the currents, voltages, and magnetic fields employed in the experiment.

III. Experimental Results and Discussion

The waveforms for the diode voltage, diode current, cavity current, and 35 GHz microwave pulses for a "typical" shot are shown in Fig. 2. The improved voltage waveform and beam quality, compared to that described in Ref. 6, have generally permitted high power microwave pulses with a duration of up to 40 nsec, nearly matching the duration of the flat portion of the high voltage pulse applied to the diode. However, the microwave pulse is subject to large shot-to-shot variation in amplitude and pulse shape. A set of measurements were conducted as a function of beam energy, magnetic field, magnetic compression ratio, and pump field amplitude, in order to find the optimum operating parameters.

Figure 3 shows a scan of the output mode of the device as a function of radius in both $|E_r|^2$ and $|E_\theta|^2$ with a cavity magnetic field of B_0=32 kG, a current of 2.5 kA, and a peak diode voltage of 1.2 MV. The estimated experimental uncertainties are ±1.5 kG on the

magnetic field, ±0.1 kA on the instantaneous current measured by the Rogowski coil, and ±0.1 MV on the diode voltage, including the effect of voltage ripple during the voltage flat-top. (The net current will be lower if current interception takes place between the Rogowski coil and the gyrotron cavity. Fluorescent screen data taken subsequent to the microwave measurements suggests that up to 20% of the current may have been intercepted under these experimental conditions.) The peak beam kinetic energy should be corrected downward by approximately 50 keV because of space charge depression, assuming an average beam α of 1.

The normalized beam radius (i.e., the ratio of the beam guiding center radius r_b to the cavity wall radius r_w) for this scan was approximately 0.725. However, there was some spread in the electron guiding centers due to beam thickness (reflecting the 1.5 mm width of the anode annulus) and finite decentering of the beam in the gyrotron cavity. This radius is close to optimum for coupling to the circularly-polarized TE_{62} mode counterrotating to the sense of electron gyration in the axial magnetic field. However, in the vicinity of 35 GHz, the beam will also couple to the $TE_{10,1}$ and TE_{14} modes, and more weakly to the TM_{23} and TM_{04} modes. The general shape of the measured profile in Fig. 3 fits reasonably well to the TE_{62} mode for both the radial and azimuthal polarizations of the rf electric field, and is similar to that of Ref. 6. The peaks at small values of the radii may be due to parasitic excitation of the TM_{04} mode. Mode purity at the output window may also be reduced by mode conversion in the 5° output taper and horn. For instance, mode conversion to the TE_{61} mode might explain the higher than expected peak in $|E_r|^2$ near the wall. A scan under

similar experimental conditions with the foilless diode with its resulting poorer quality beam revealed a higher content of undesired modes.

For the data of Fig. 3, the measured mode pattern can be used to calculate the total gyrotron power by integrating over the output window, and correcting for the measured losses in the detection system. This procedure has been described in detail elsewhere.[6] The power estimate, which is based on the average of several shots per position in the scan, is 160 MW. Subsequent data taken at a fixed position has shown the total equivalent output power to reach a single-shot peak value of 275 MW, with 250 MW being measured on several occasions. The single shot efficiencies, based on the Rogowski coil measurements of beam current, varied from 9 to 14%. Based on error bars in the averaging process and in the calibration of the various multiplicative factors, the overall uncertainty of the power values is estimated to be less than 3 dB.

Figure 4 shows starting current and output isopower curves for the gyrotron interaction with the counterrotating TE_{62} mode, calculated from a steady-state model[8] for B_0=32 kG. The beam current is assumed to scale as $V^{1.5}$ with a maximum value of 2.5 kA at 1.15 MV, and the beam α is assumed to scale linearly with V, with a maximum value of α=1 at 1.15 MV. The starting current and isopower curves are calculated assuming a half-sinusoidal rf-field profile along the cavity axis with a length of 3.5 cm and a hollow beam with a radius, normalized to the cavity wall radius, of 0.725. The dotted line models the behavior of the electron beam current during the rise of the voltage waveform. The effect of increasing voltage on the coupling to this mode may be inferred from this figure. As the voltage (and current) rise to their flat-top values, the interaction will begin at the left of the figure, where

the beam line crosses the starting current line labelled I_{thr}, and then progressively tune to higher powers as the voltage and current continue to rise. The line ends at 2.5 kA and 1.15 MeV, and corresponds to predicted operation outside of the starting current curve, i.e. in the "hard excitation" regime, with a peak power of approximately 400 MW. Aside from the peak power predictions, this simulation is in reasonable agreement with the experimental observations.

In order to better understand the time-dependent nature of the gyrotron operation, as illustrated in Fig. 2, we have carried out a set of slow-time-scale single-mode time-dependent simulations of gyrotron operation for the approximate experimental conditions corresponding to the measurements shown in Fig. 3. Figure 5 shows a series of time-dependent simulations of the gyrotron operation,[9] employing a simulated VEBA voltage waveform that models the leading edge of the pulse, the duration of the approximately flat portion of the voltage waveform, and a "typical" short-duration voltage "spike" during the "flat-top." These simulations employ the same sinusoidal rf-field profile used for the steady-state simulations, and assume the same dependence of current and beam α on voltage. For the four runs shown, only the magnetic field was varied. At the lowest magnetic field, B_0=31 kG (Fig. 5a), the microwave signal occurs only during the rise and fall of the voltage waveform, and there is no interaction at the voltage flat-top. The next case (Fig. 5b), for B_0=32 kG, corresponds to the steady-state simulations of Fig. 4. In this case, the microwave signal grows substantially during the leading edge of the voltage pulse, and persists up to the voltage flat-top. Figure 5b demonstrates that the full voltage of the flat-top, corresponding to the upper end point of the beam line in Fig. 4, results in a highly detuned state of the gyrotron interaction, corresponding

to "hard excitation." This is evident because the short-duration voltage spike modeled at approximately 45 nsec detunes the interaction further, causing the output power to fall off dramatically, and the power does not begin to recover until the voltage falls below the flat-top voltage. This case agrees well with the steady-state simulation of Fig. 4, and the peak power predicted by this simulation exceeds the best experimental value by approximately a factor of two, as in Fig. 4. At B_0=33 kG (Fig. 5c), the voltage flat-top no longer corresponds to hard excitation, since the microwave signal falls off during the voltage spike, but then recovers during the remainder of the flat-top. Finally, at B_0=34 kG (Fig. 5d), the simulation shows the microwave power to follow the voltage signal for the duration of its flat portion including the voltage spike, and the power actually increases during the voltage spike.

For the assumed voltage waveform, the best agreement between the experimental microwave signals and the predictions of the single-mode time-dependent code, as a function of magnetic field, occurs at the experimental value of B_0=32 kG. However, the experimental values have error bars, as noted previously. In addition, the predictions of the time-dependent simulation depend in part on the exact shape of the axial rf-field profile assumed for the interaction, and small variations in the assumed length of the sinusoidal profile, or in substituting an approximately equivalent gaussian profile for the sinusoid, will change the required values of the externally-applied axial magnetic field by one to two kG. The time-dependent simulations of Fig. 5 suggest that the microwave signal should last longer and reach higher power as the magnetic field is increased beyond the best experimental value of B_0=32 kG. In general, this is not observed in the laboratory. A possible explanation for this experimental observation lies in the area of mode competition. Specifically, as the magnetic

field is increased, it becomes increasingly probable that a higher frequency mode will start oscillation during the rise of the voltage waveform, and will interfere with the start-up of the TE_{62} mode at 35 GHz. The most likely competing mode in this situation is the counterrotating TE_{72} mode. Time-dependent simulations carried out for the TE_{72} mode indicate that it should begin to compete with the start-up of the TE_{62} mode at approximately 34 kG. A thorough analysis of the effects of mode competition and other transient phenomena on the operation of a high voltage gyrotron would require the use of true multimode simulations, such as the fast-time-scale particle-in-cell simulations carried out by A.T. Lin et al. for the parameters of Ref. 6.[10]

In summary, a 35 GHz gyrotron oscillator has successfully operated at voltages exceeding 1 MeV and currents of several kiloamps to produce peak power levels of up to a quarter of a GW in a TE_{62} mode at peak efficiencies exceeding 10%. Its interaction efficiency has been improved compared to earlier experiments by the use of an apertured diode, in place of the foilless diode configuration used previously, which has allowed better control of the current injected into the gyrotron and better beam quality. By comparison, an earlier TE_{62} experiment operating at approximately 800 keV and 1.6 kA at the same frequency in the same TE_{62} mode achieved 100 MW at 8% efficiency. Overall experimental operation is in general agreement with the predictions of theory, with the best experimental powers within a factor of two of the theoretical predictions.

Acknowledgments

This work was supported in part by the Office of Naval Research. This work was also supported in part by the Office of Innovative Science and Technology of the Strategic Defense Initiative Organization and managed by the Harry Diamond Laboratories.

References

1. A.W. Fliflet, Naval Research Laboratory Memorandum Report 5598, 1985. Also available as National Technical Information Service Document No. ADA-157476.
2. S.N. Voronkov, V.I. Krementsov, P.S. Strelkov, and A.G. Shkvarunets, Zh. Tekh. Fiz. 52, 106 (1982) [Sov. Phys.-Tech. Phys. 27, 68 (1982)]. Also, V.V. Bogdanov, S.N. Voronkov, V.I. Krementsov, P.S. Strelkov, V.Yu. Shafer, and A.G. Shkvarunets, Zh. Tekh. Fiz. 53, 106 (1983) [Sov. Phys.-Tech. Phys. 28, 61 (1983)].
3. R.M. Gilgenbach, J.G. Wang, J.J. Choi, C.A. Outten, and T.A. Spencer, in Conference Digest of the Thirteenth International Conference on Infrared and Millimeter Waves, edited by R.J. Temkin (SPIE, Bellingham, WA, 1988), pp. 362-363.
4. A.D.R. Phelps, T. Garvey, and A.S. Hasaani, Int. J. Electron. 57, 1141 (1984).
5. S.H. Gold, A.W. Fliflet, W.M. Manheimer, W.M. Black, V.L. Granatstein, A.K. Kinkead, D.L. Hardesty, and M. Sucy, IEEE Trans. Plasma Sci. PS-13, 374 (1985).
6. S.H. Gold, A.W. Fliflet, W.M. Manheimer, R.B. McCowan, W.M. Black, R.C. Lee, V.L. Granatstein, A.K. Kinkead, D.L. Hardesty, and M. Sucy, Phys. Fluids 30, 2226 (1987).
7. S.H. Gold, A.W. Fliflet, W.M. Manheimer, R.B. McCowan, R.C. Lee, V.L. Granatstein, D.L. Hardesty, A.K. Kinkead, and M. Sucy, IEEE Trans. Plasma Sci. PS-16, 142 (1988).
8. A.W. Fliflet, M.E. Read, K.R. Chu, and R. Seeley, Int. J. Electron. 53, 505 (1982).
9. A.W. Fliflet and W.M. Manheimer, Phys. Rev. A, to be published.
10. A.T. Lin, C.-C. Lin, Z.H. Yang, K.R. Chu, A.W. Fliflet, and S.H. Gold, IEEE Trans. Plasma Sci. 16, 135 (1988).

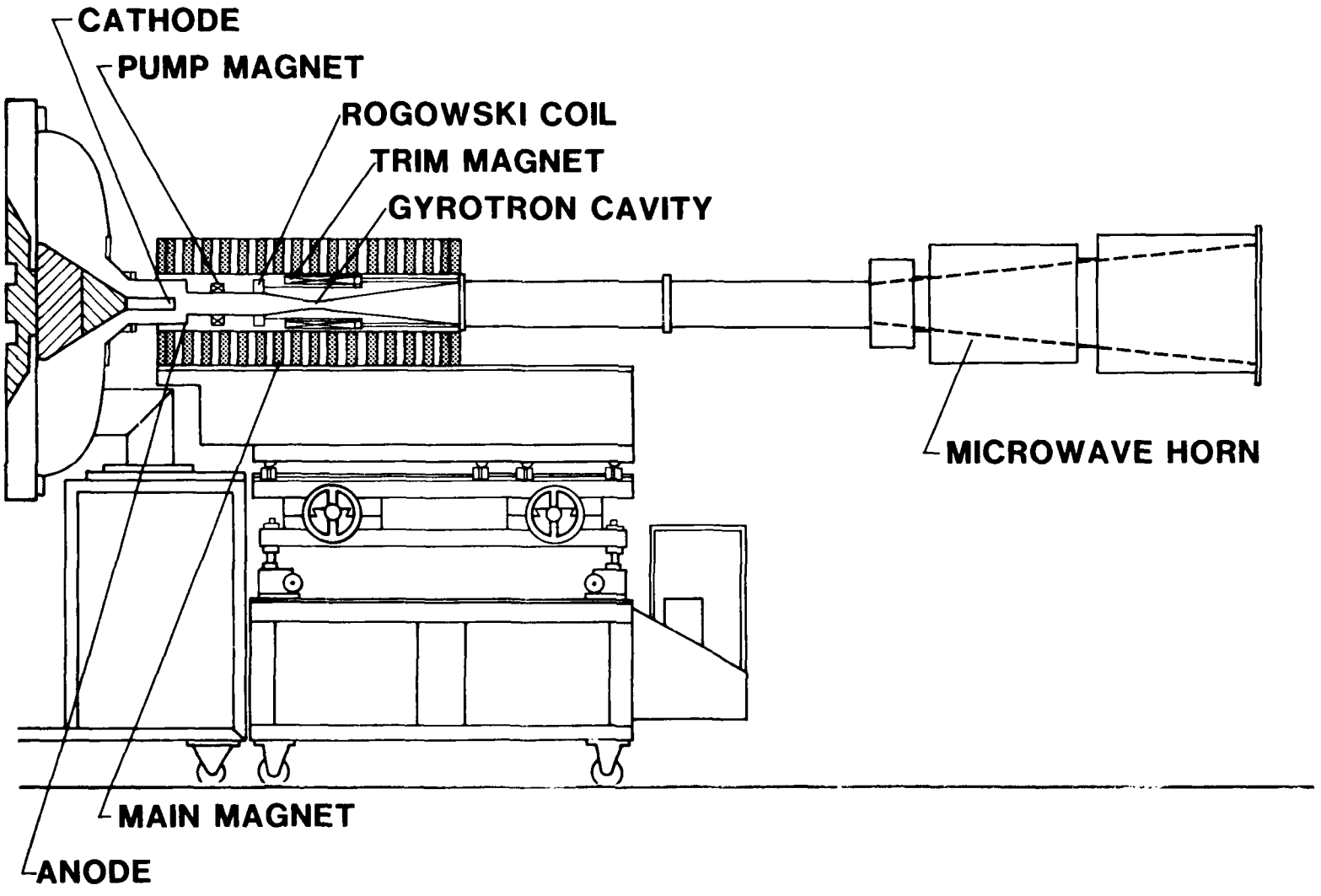

Fig. 1. Schematic diagram of the high voltage gyrotron experimental setup.

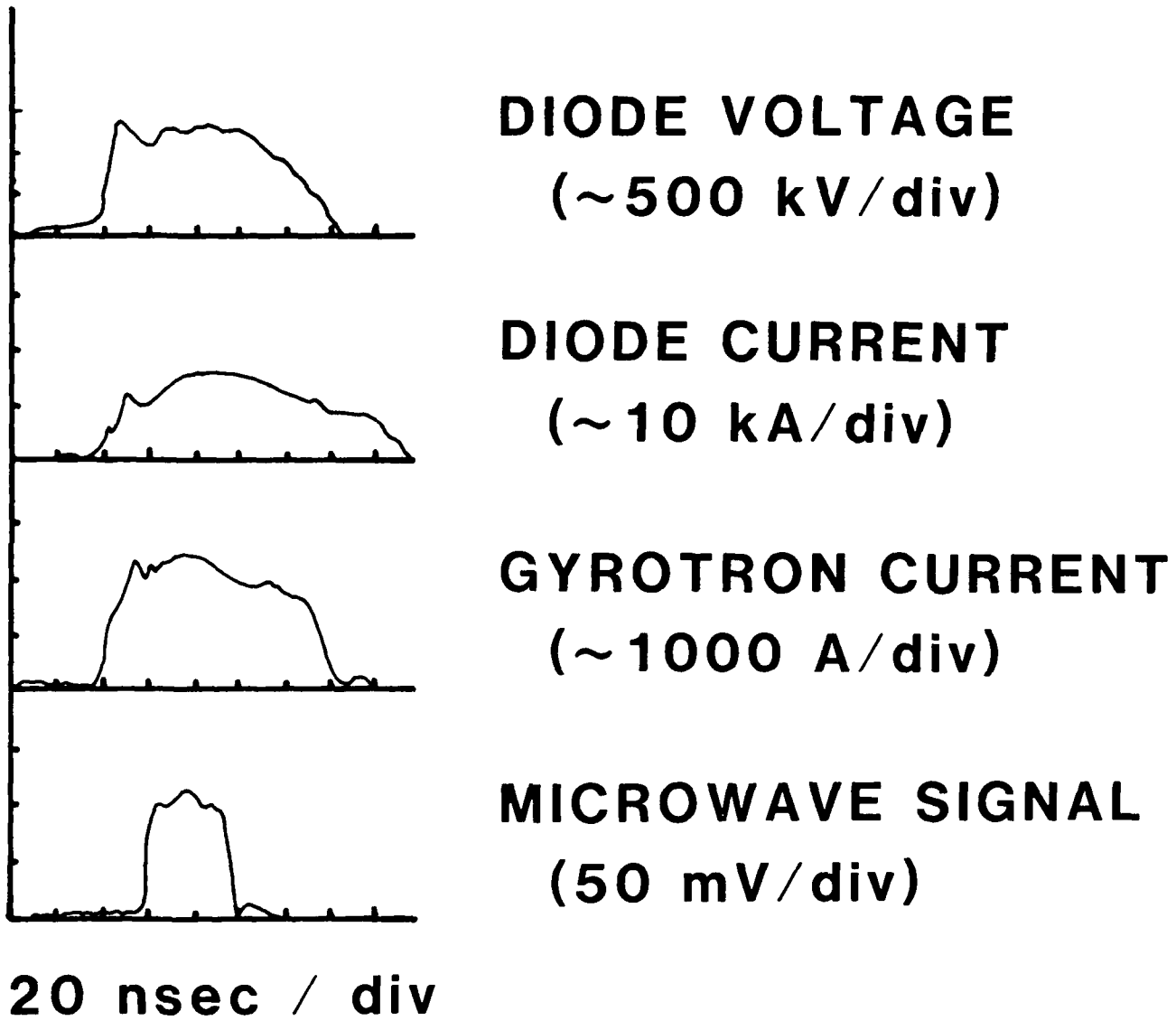

Fig. 2. Measured experimental waveforms as a function of time.

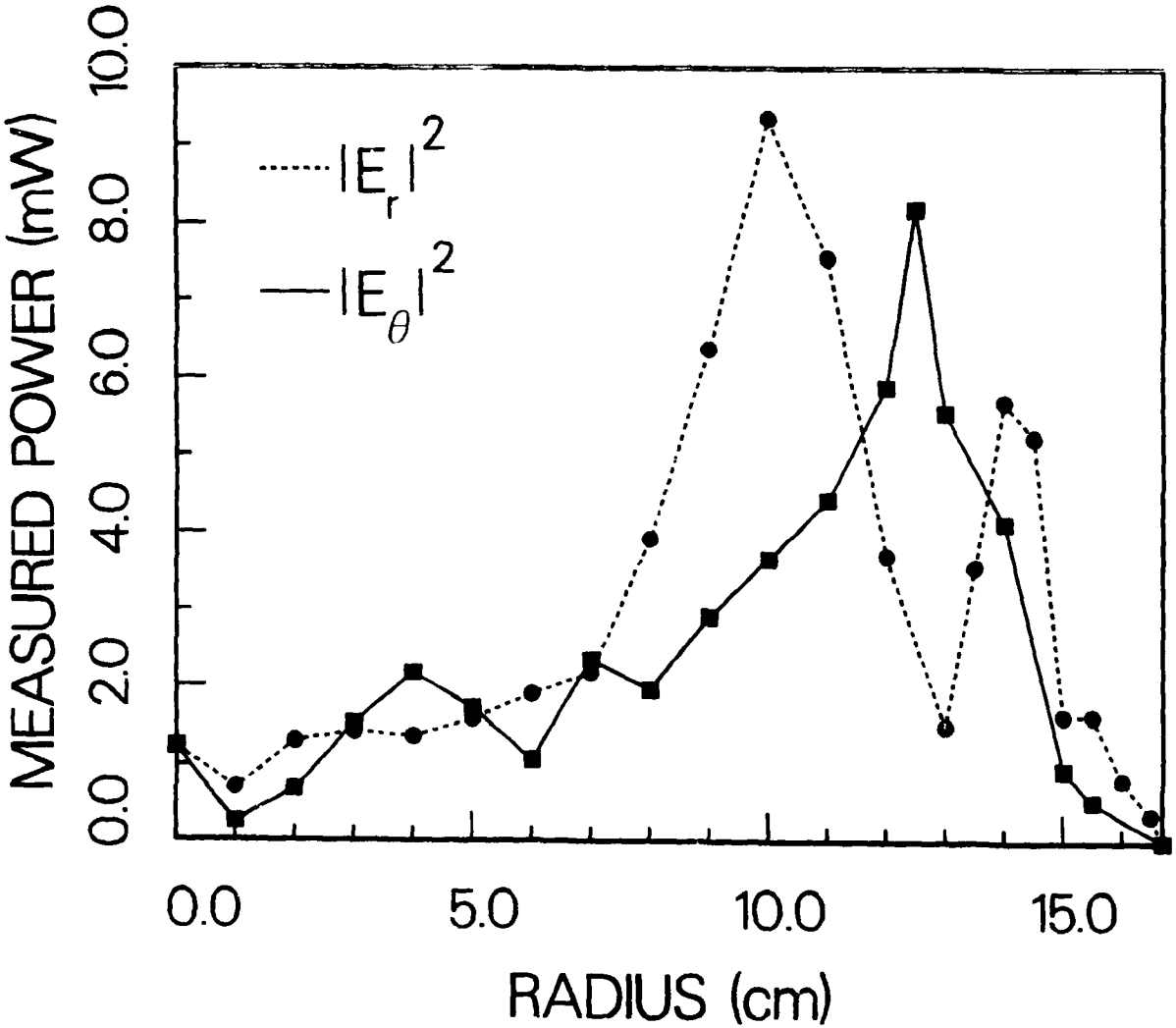

Fig. 3. Scan of output power versus radius, in both radial and azimuthal polarizations, across the output window.

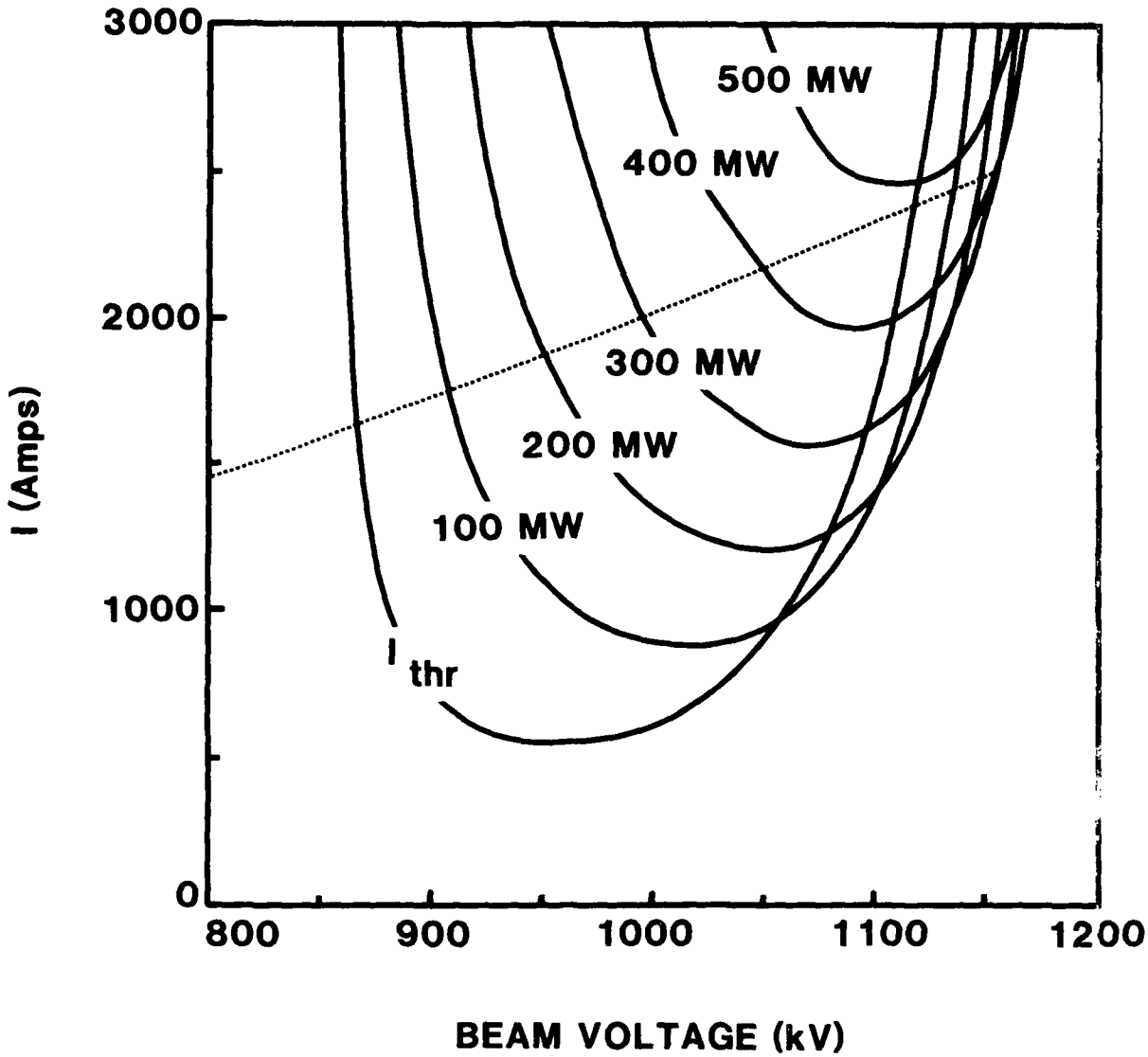

Fig. 4. Gyrotron starting current and isopower curves for the counterrotating TE_{62} mode as a function of beam voltage, assuming r_b/r_w=0.725, B_0=32 kG, and that the beam α is proportional to V, with α=1 at 1.15 MeV. A beam line is included, with the current assumed to scale as $V^{1.5}$, with a maximum value I=2.5 kA at 1.15 MeV.

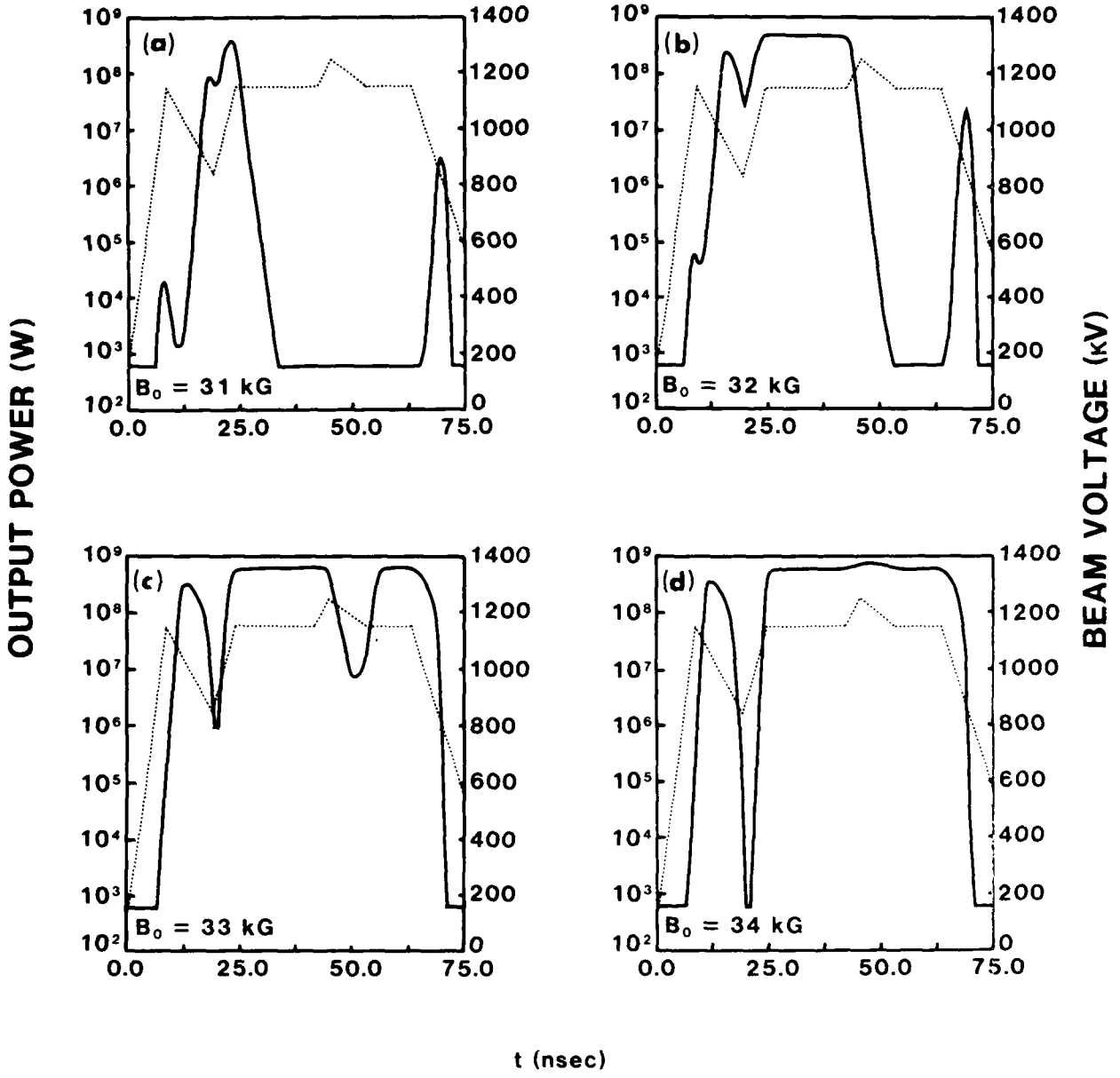

Fig. 5. Single-mode slow-time-scale time-dependent simulations of gyrotron operation in the counterrotating TE_{62} mode for a simulated VEBA voltage waveform, assuming r_b/r_w=0.725, $\alpha \propto V$ with α=1 at 1.15 MeV, and $I \propto V^{1.5}$ with I=2.5 kA at 1.15 MeV. Runs with four values of B_0 are shown: (a) 31 kG, (b) 32 kG, (c) 33 kG, and (d) 34 kG.

4740 DISTRIBUTION LIST

Air Force Avionics Laboratory
AFWAL/AADM-1
Wright/Patterson AFB, Ohio 45433
Attn: Walter Friez — 1 copy

Air Force Office of
Scientific Research
Bolling AFB
Washington, D.C. 20332
Attn: H. Schlossberg — 1 copy

Air Force Weapons Lab
Kirkland AFB
Albuquerque, New Mexico 87117
Attn: Dr. William Baker — 2 copies

Columbia University
520 West 120th Street
Department of Electrical Engineering
New York, N.Y. 10027
Attn: Dr. S.P. Schlesinger — 1 copy
A. Sen — 1 copy

Columbia University
520 West 120th Street
Department of Applied Physics
and Nuclear Engineering
New York, New York 10027
Attn: T.C. Marshall — 1 copy
R. Gross — 1 copy

Cornell University
School of Applied and Engineering Physics
Ithica, New York 14853
Attn: Prof. Hans H. Fleischmann — 1 copy
John Nation — 1 copy
R. N. Sudan — 1 copy

Dartmouth College
18 Wilder, Box 6127
Hanover, New Hampshire 03755
Attn: Dr. John E. Walsh — 1 copy

Department of Energy
The Pentagon
Washington, D.C. 20545
Attn: C. Finfgeld/ER-542, GTN — 1 copy
T.V. George/ER-531, GTN — 1 copy
D. Crandall/ER-55, GTN — 1 copy

Defense Advanced Research Project Agency/DEO
1400 Wilson Blvd.
Arlington, Virginia 22209
Attn: Dr. S. Shey — 1 copy
Dr. L. Buchanan — 1 copy

Defense Communications Agency
Washington, D.C. 20305
Attn: Dr. Pravin C. Jain
Assistant for Communications
Technology — 1 copy

Defense Nuclear Agency
Washington, D.C. 20305
Attn: Mr. J. Farber — 1 copy
Dr. Leon Wittwer (RAAE) — 5 copies

Defense Technical Information Center
Cameron Station
5010 Duke Street
Alexandria, Virginia 22314 — 2 copies

General Automics
13-260
Box 85608
San Diego, CA 92138
ATTN: Dr. J. Doane — 1 copy

Georgia Tech. EES-EOD
Baker Building
Atlanta, Georgia 30332
Attn: Dr. James J. Gallagher — 1 copy

Hanscomb Air Force Base
Stop 21, Massachusetts 01731
Attn: Lt. Rich Nielson/ESD/INK — 1 copy

Hughes Aircraft Co.
Electron Dynamics Division
3100 West Lomita Boulevard
Torrance, California 90509
Attn: J. Christiansen — 1 copy
J.J. Tancredi — 1 copy

KMS Fusion, Inc.
3941 Research Park Dr.
P.O. Box 1567
Ann Arbor, Michigan 48106
Attn: S.B. Segall — 1 copy

Lawrence Livermore National Laboratory
P.O. Box 808
Livermore, California 94550
Attn: Dr. D. Prosnitz — 1 copy
Dr. T.J. Orzechowski — 1 copy
Dr. J. Chase — 1 copy

Los Alamos Scientific Laboratory
P.O. Box 1663, AT5-827
Los Alamos, New Mexico 87545

Attn: Dr. T.J.T. Kwan	1 copy
Dr. L. Thode	1 copy
Dr. C. Brau	1 copy
Dr. R. R. Bartsch	1 copy

Massachusetts Institute of Technology
Department of Physics
Cambridge, Massachusetts 02139

Attn: Dr. G. Bekefi/36-213	1 copy
Dr. M. Porkolab/NW 36-213	1 copy
Dr. R. Davidson/NW 16-206	1 copy
Dr. A. Bers/NW 38-260	1 copy
Dr. K. Kreischer	1 copy

Massachusetts Institute of Technology
167 Albany St., N.W. 16-200
Cambridge, Massachusetts 02139

Attn: Dr. R. Temkin/NW 14-4107	1 copy

Spectra Technologies
2755 Northup Way
Bellevue, Washington 98004

Attn: Dr. J.M. Slater	1 copy

Mission Research Corporation
Suite 201
5503 Cherokee Avenue
Alexandria, Virginia 22312

Attn: Dr. M. Bollen	1 copy
Dr. Tom Hargreaves	1 copy

Mission Research Corporation
1720 Randolph Road, S.E.
Albuquerque, New Mexico 87106

Attn: Mr. Brendan B. Godfrey	1 copy

SPAWAR
Washington, D.C. 20363

Attn: E. Warden	
Code PDE 106-3113	1 copy
G. Bates	
PMW 145	1 copy

Naval Research Laboratory

Addressee: Attn: Name/Code	
Code 1001 - T. Coffey	1 copy
Code 1220 - Security	1 copy
Code 2628 - TID Distribution	22 copies
Code 4000 - W. Ellis	1 copy
Code 4700 - S. Ossakow	26 copies

Code 4700.1 - A.W. Ali	1 copy
Code 4710 - C. Kapetanakos	1 copy
Code 4740 - Branch Office	25 copies
Code 4740 - W. Black	1 copy
Code 4740 - A. Fliflet	1 copy
Code 4740 - S. Gold	1 copy
Code 4740 - A. Kinkead	1 copy
Code 4740 - W.M. Manheimer	1 copy
Code 4740 - M. Rhinewine	1 copy
Code 4770 - G. Cooperstein	1 copy
Code 4790 - B. Hui	1 copy
Code 4790 - C.M. Hui	1 copy
Code 4790 - Y.Y. Lau	1 copy
Code 4790 - P. Sprangle	1 copy
Code 5700 - L.A. Cosby	1 copy
Code 6840 - S.Y. Ahn	1 copy
Code 6840 - A. Ganguly	1 copy
Code 6840 - R.K. Parker	1 copy
Code 6840 - N.R. Vanderplaats	1 copy
Code 6850 - L.R. Whicker	1 copy
Code 6875 - R. Wagner	1 copy

Naval Sea Systems Command
Department of the Navy
Washington, D.C. 20362
Attn: Commander George Bates
PMS 405-300 — 1 copy

Northrop Corporation
Defense Systems Division
600 Hicks Rd.
Rolling Meadows, Illinois 60008
Attn: Dr. Gunter Dohler — 1 copy

Oak Ridge National Laboratory
P.O. Box Y
Mail Stop 3
Building 9201-2
Oak Ridge, Tennessee 37830
Attn: Dr. A. England — 1 copy

Office of Naval Research
800 N. Quincy Street
Arlington, Va. 22217
Attn: Dr. C. Roberson — 1 copy
Dr. W. Condell — 1 copy
Dr. T. Berlincourt — 1 copy

Office of Naval Research
1030 E. Green Street
Pasadena, CA 91106
Attn: Dr. R. Behringer — 1 copy

Optical Sciences Center
University of Arizona
Tucson, Arizona 85721
Attn: Dr. Willis E. Lamb, Jr. — 1 copy

Physics International
2700 Merced Street
San Leandro, California 94577
Attn: Dr. J. Benford — 1 copy

Physical Science Inc.
603 King Street
Alexandria, VA 22314
ATTN: M. Read — 1 copy

Princeton Plasma
Plasma Physics Laboratory
James Forrestal Campus
P.O. Box 451
Princeton, New Jersey 08544
Attn: Dr. H. Hsuan — 2 copies
Dr. D. Ignat — 1 copy
Dr. H. Furth — 1 copy
Dr. P. Efthimion — 1 copy
Dr. F. Perkins — 1 copy

Quantum Institute
University of California
Santa Barbara, California 93106
Attn: Dr. L. Elias — 1 copy

Raytheon Company
Microwave Power Tube Division
Foundry Avenue
Waltham, Massachusetts 02154
Attn: N. Dionne — 1 copy

Sandia National Laboratories
ORG. 1231, P.O. Box 5800
Albuquerque, New Mexico 87185
Attn: Dr. Thomas P. Wright — 1 copy
Mr. J.E. Powell — 1 copy
Dr. J. Hoffman — 1 copy
Dr. W.P. Ballard — 1 copy
Dr. C. Clark — 1 copy

Science Applications, Inc.
1710 Goodridge Dr.
McLean, Virginia 22102
Attn: Adam Drobot — 1 copy
P. Vitrello — 1 copy
D. Bacon — 1 copy
C. Menyuk — 1 copy

Stanford University
High Energy Physics Laboratory
Stanford, California 94305
Attn: Dr. T.I. Smith — 1 copy

TRW, Inc.
Redondo Beach, California 90278
Attn: Dr. H. Boehmer — 1 copy
Dr. T. Romisser — 1 copy
Dr. Z. Guiragossian — 1 copy

University of California
Physics Department
Irvine, California 92717
Attn: Dr. G. Benford — 1 copy
Dr. N. Rostoker — 1 copy

University of California
Department of Physics
Los Angeles, CA 90024
Attn: Dr. A.T. Lin — 1 copy
Dr. N. Luhmann — 1 copy
Dr. D. McDermott — 1 copy

University of Maryland
Department of Electrical Engineering
College Park, Maryland 20742
Attn: Dr. V. L. Granatstein — 1 copy
Dr. W. W. Destler — 1 copy

University of Maryland
Laboratory for Plasma and Fusion
Energy Studies
College Park, Maryland 20742
Attn: Dr. Tom Antonsen — 1 copy
Dr. John Finn — 1 copy
Dr. Jhan Varyan Hellman — 1 copy
Dr. Baruch Levush — 1 copy
Dr. John McAdoo — 1 copy
Dr. Edward Ott — 1 copy

University of Tennessee
Dept. of Electrical Engr.
Knoxville, Tennessee 37916
Attn: Dr. I. Alexeff — 1 copy

University of New Mexico
Department of Physics and Astronomy
800 Yale Blvd, N.E.
Albuquerque, New Mexico 87131
Attn: Dr. Gerald T. Moore — 1 copy

University of Utah
Deparment of Electrical Engineering
3053 Merrill Engineering Bldg.
Salt Lake City, Utah 84112
Attn: Dr. Larry Barnett — 1 copy
Dr. J. Mark Baird — 1 copy

U. S. Naval Academy
Annapolis, Maryland 21402-5021 — 1 copy

U. S. Army
Harry Diamond Labs
2800 Powder Mill Road
Adelphi, Maryland 20783-1145
Attn: Dr. Howard Brandt — 1 copy
Dr. Edward Brown — 1 copy
Dr. Stuart Graybill — 1 copy

Varian Associates
611 Hansen Way
Palo Alto, California 94303
Attn: Dr. H. Jory — 1 copy
Dr. Kevin Felch — 1 copy
Dr. A. Salop — 1 copy

Varian Eimac San Carlos Division
301 Industrial Way
San Carlos, California 94070
Attn: C. Marshall Loring — 1 copy

Yale University
Applied Physics
Madison Lab
P.O. Box 2159
Yale Station
New Haven, Connecticut 06520
Attn: Dr. I. Bernstein — 1 copy